# Supplementary Material for

## Prussian Blue Analogue-Derived Fe-Doped $CoS_2$ Nanoparticles Confined in Bayberry-Like N-Doped Carbon Spheres as Anodes for Sodium-Ion Batteries

Jiajia Hu, Cheng Liu, Chen Cai, Qianqian Sun, Mixue Lu, Zhujun Yao, and Yefeng Yang*

*School of Materials Science and Engineering, Zhejiang Sci-Tech University, Hangzhou 310018, China*

* *Correspondence: yangyf@zstu.edu.cn; Tel.: +86-571 8684 5569*

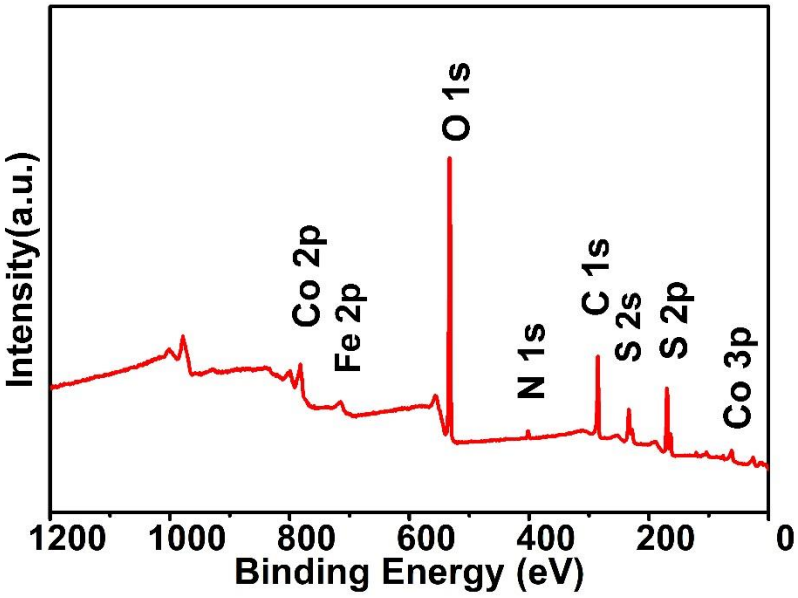


**Figure S1.** XPS survey spectrum of the Fe-$CoS_2$/NC-3.

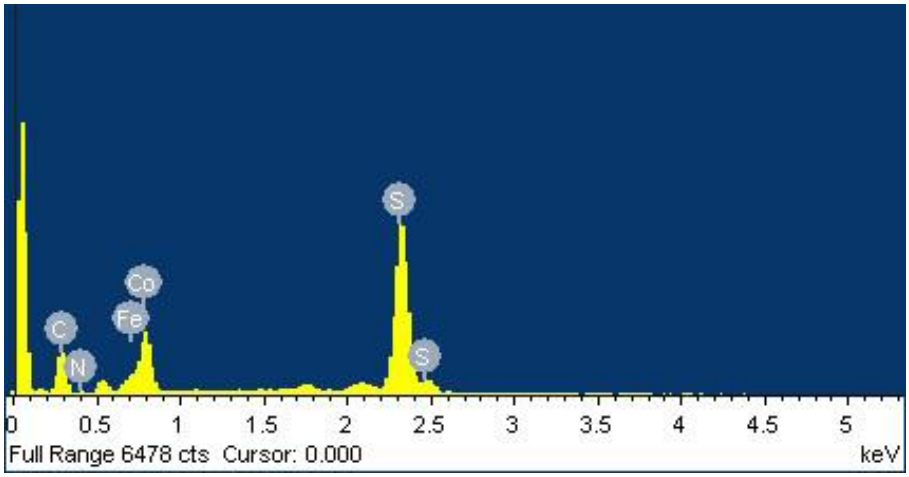


**Figure S2.** EDS spectrum of the Fe-$CoS_2$/NC-3 sample.

**Table S1.** The element contents in Fe-$CoS_2$/NC-3 measured by EDS measurement.

| Element | Co | Fe | S | C | N | Total |
|---|---|---|---|---|---|---|
| Contents (wt%) | 30.0 | 3.7 | 33.0 | 31.3 | 2.1 | 100.0 |

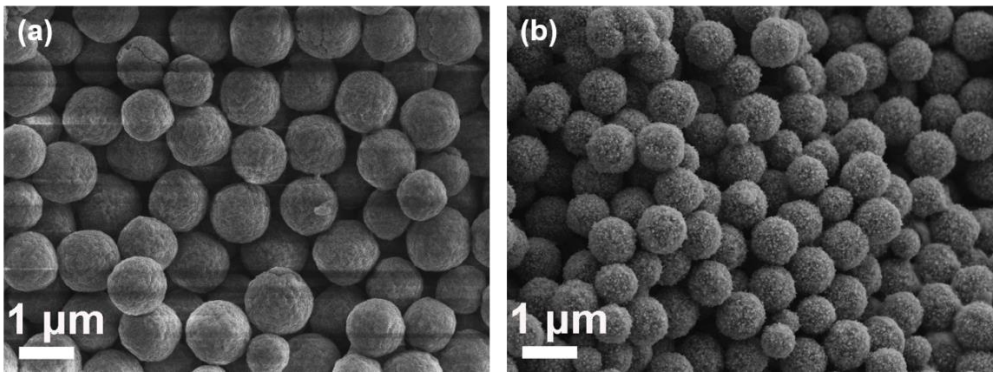


**Figure S3.** SEM images of (a) ZnCo-PBA precursor spheres, and (b) $CoS_2$/NC spheres.

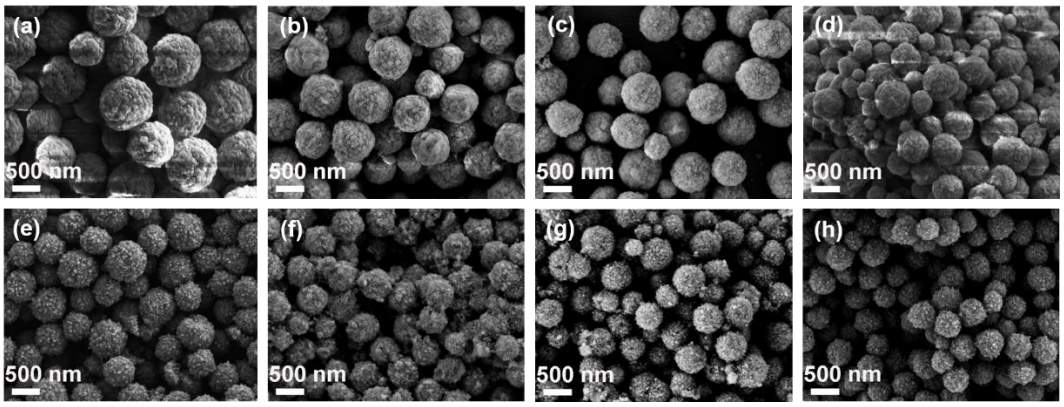


**Figure S4.** SEM images of (a) FeZnCo-PBA-1, (b) FeZnCo-PBA-2, (c) FeZnCo-PBA-3, (d) FeZnCo-PBA-4 precursor spheres, (e) Fe-$CoS_2$/NC-1, (f) Fe-$CoS_2$/NC-2, (g) Fe-$CoS_2$/NC-3, and (h) Fe-$CoS_2$/NC-4 hybrid spheres.

**Table S2.** The average diameters of precursors and obtained samples derived from the reactions with different introduced amounts of $FeCl_3$.

| Precursors | Average diameter | Samples | Average diameter |
|---|---|---|---|
| ZnCo-PBA | 1000 nm | $CoS_2$/NC | 810 nm |
| FeZnCo-PBA-1 | 723 nm | Fe-$CoS_2$/NC-1 | 482 nm |
| FeZnCo-PBA-2 | 583 nm | Fe-$CoS_2$/NC-2 | 478 nm |
| FeZnCo-PBA-3 | 572 nm | Fe-$CoS_2$/NC-3 | 450 nm |
| FeZnCo-PBA-4 | 496 nm | Fe-$CoS_2$/NC-4 | 408 nm |

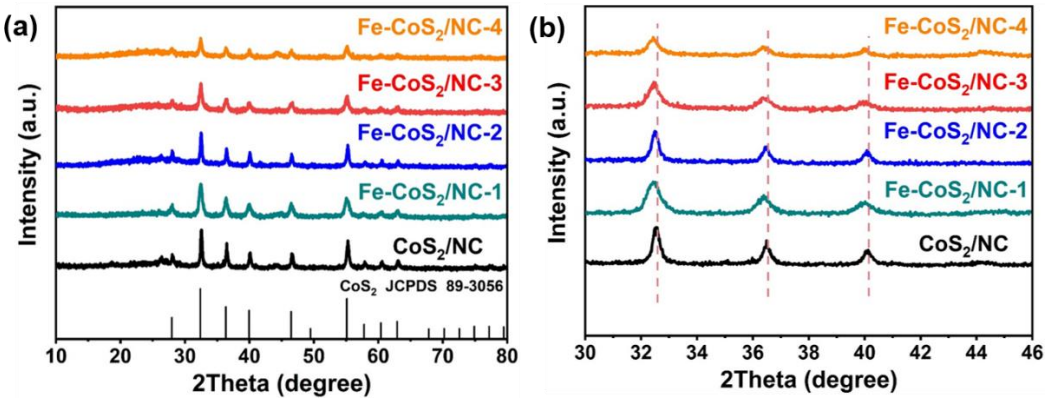


**Figure S5.** (a) XRD patterns of $CoS_2$/NC, Fe-$CoS_2$/NC-1, Fe-$CoS_2$/NC-2, Fe-$CoS_2$/NC-3, and Fe-$CoS_2$/NC-4 spheres in the range of 10-80°, and (b) zoom view of (a) in the range of 30-46°.

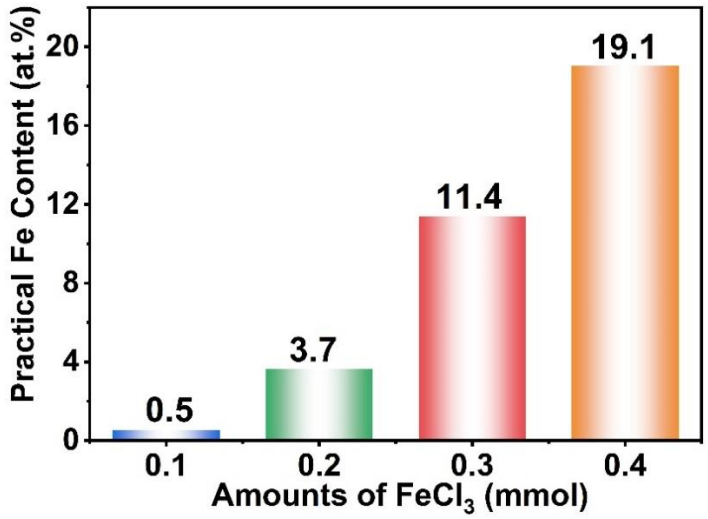


**Figure S6.** The practical Fe contents in products and the feeding Fe contents in the starting materials of Fe-$CoS_2$/NC-1, Fe-$CoS_2$/NC-2, Fe-$CoS_2$/NC-3, and Fe-$CoS_2$/NC-4.

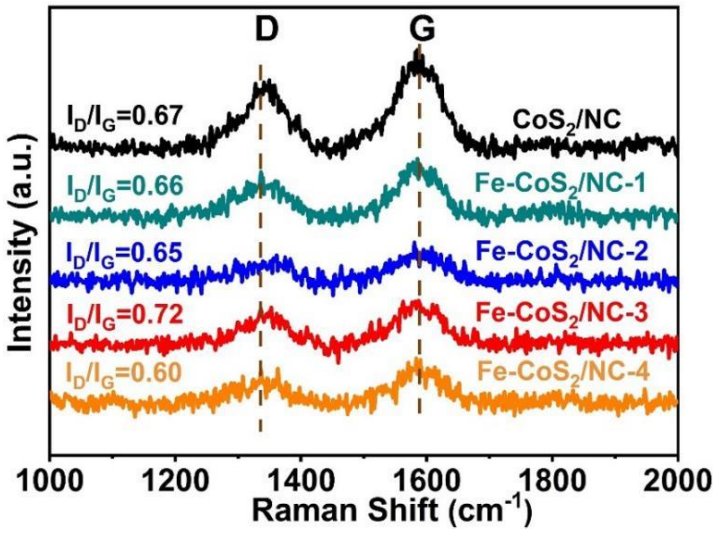


**Figure S7.** Raman spectra of $CoS_2$/NC, Fe-$CoS_2$/NC-1, Fe-$CoS_2$/NC-2, Fe-$CoS_2$/NC-3, and Fe-$CoS_2$/NC-4.

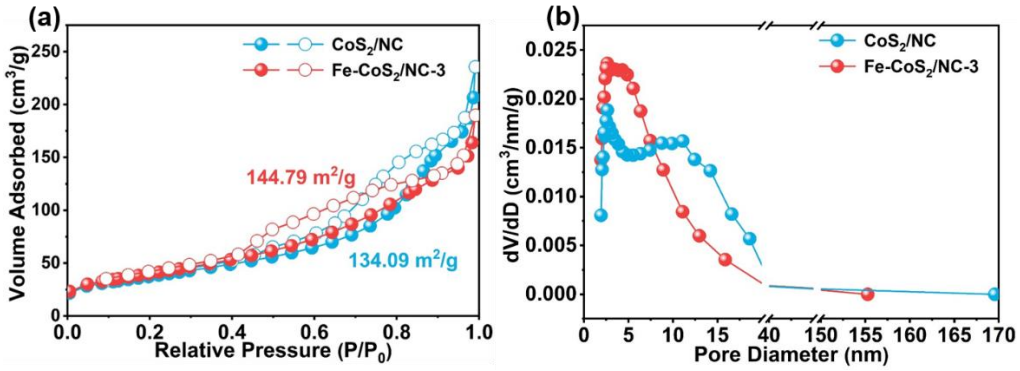


**Figure S8.** (a) $N_2$ adsorption-desorption isotherms curves of $CoS_2$/NC and Fe-$CoS_2$/NC-3, and (b) pore size distributions of the $CoS_2$/NC and Fe-$CoS_2$/NC-3.

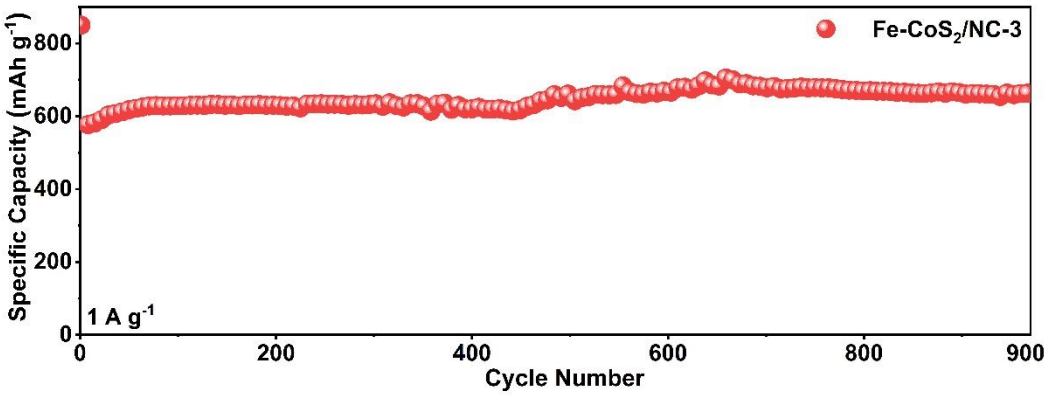


**Figure S9.** Long-term cycling performance of the Fe-$CoS_2$/NC-3 electrode.

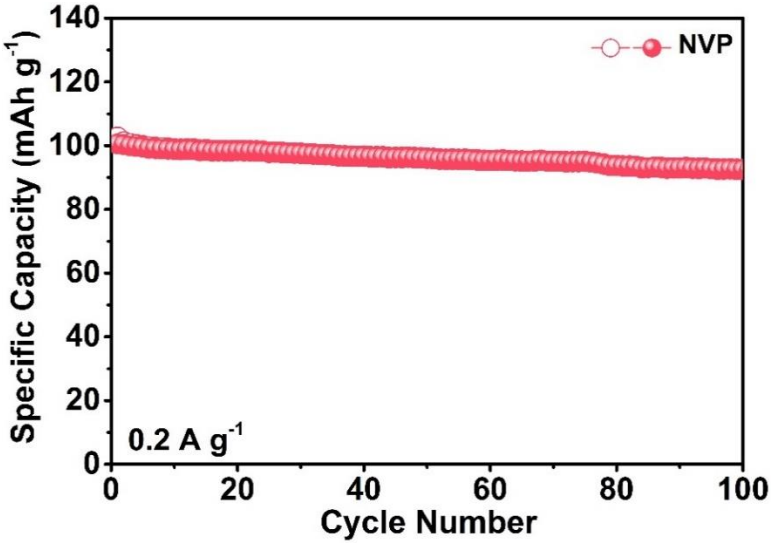


**Figure S10.** Cycling performance of NVP at current density of 0.2 A $g^{-1}$.

**Table S3**. Comparison of electrochemical performance of Fe-$CoS_2$/NC-3//NVP full SIBs in this work with previously reported metal sulfide-NVP full SIBs.

| Anode | Cathode | Capacity/current density/cycles (mAh $g^{-1}$/A $g^{-1}$/n) | Energy density/current density (Wh $kg^{-1}$/A $g^{-1}$) | Power density (W $kg^{-1}$) | Ref. |
|---|---|---|---|---|---|
| Fe-$CoS_2$/NC-3 | NVP | 313/0.5/60 | 102/0.2 | 74 | This work |
| SnS/$Fe_2O_3$-G | NVP | 51/1/200 | 141.8/0.2 | 60 | [75] |
| FeS@NCG | NVP@C | 308/0.6/150 | 218/0.6 | – | [76] |
| $FeS_2$@G@CNF | NVP@C | 102/1C/100 | 169/1C | 88 | [77] |
| $V_3S_4$@CNF | NVP/C | 365/0.1/20 | 400/0.1 | – | [78] |
| $Ti_3C_2T_x$/$FeS_2$ | NVP | 365/3/200 | 80/5 | – | [79] |
| Cu-$SnS_2$@NC | NVP | 223/0.5/50 | 233 | 240 | [80] |
| $NiS_2$@$SnS_2$ | NVP | 628/0.5/150 | 274 | 52.1 | [73] |